Neutrino Mass Ordering Obscured by Nonstandard Interactions

Francesco Capozzi[,1,*] Sabya Sachi Chatterjee[,2,†] and Antonio Palazzo[3,4,‡]

[1]*Max-Planck-Institut für Physik (Werner-Heisenberg-Institut), Föhringer Ring 6, 80805 München, Germany*
[2]*Institute for Particle Physics Phenomenology, Department of Physics, Durham University, Durham, DH1 3LE, United Kingdom*
[3]*Dipartimento Interateneo di Fisica "Michelangelo Merlin," Via Amendola 173, 70126 Bari, Italy*
[4]*Istituto Nazionale di Fisica Nucleare, Sezione di Bari, Via Orabona 4, 70126 Bari, Italy*

One of the major open questions in particle physics is the issue of the neutrino mass ordering (NMO). The current data of the two long-baseline experiments NOνA and T2K, interpreted in the standard three-flavor scenario, provide a $\sim 2.4\sigma$ indication in favor of the normal neutrino mass ordering. We show that such an indication is completely washed out if one assumes the existence of neutral-current nonstandard interactions (NSI) of the flavor changing type involving the $e - \tau$ flavors. This implies that the claim for a discovery of the NMO will require a careful consideration of the impact of hypothetical NSI.

Introduction.—The neutrino mass ordering (NMO) is one of the most important unknown properties in particle physics. Its determination is crucial for flavor model building and has direct implications for the efforts to determine the nature of the neutrino (Dirac vs Majorana) with neutrinoless double-beta decay searches. We recall that in the three-flavor scheme there are three mass eigenstates ν_i with masses m_i ($i = 1, 2, 3$), three mixing angles θ_{12}, θ_{13}, θ_{13}, and one charge parity (*CP*)-phase δ. The mass ordering is defined to be normal (NO) if $m_3 > m_{1,2}$ or inverted (IO) if $m_3 < m_{1,2}$. A rich dedicated program of experiments is underway to nailing down the NMO with accelerator, atmospheric, and reactor neutrinos. Quite interestingly the two running long-baseline experiments (LBL) NOνA and T2K, in combination with the reactor data sensitive to θ_{13}, already provide a $\sim 2\sigma$ indication in favor of NO [1]. This trend is independently corroborated by the Super-Kamiokande atmospheric data [2]. As a consequence the most recent global fits display a preference for NO at the remarkable $\sim 3\sigma$ level [3–5].

It is important to underline that such an indication is established within the standard three-flavor scheme, and its validity in scenarios involving physics beyond the standard model is unknown. In this work we focus on neutral current nonstandard neutrino interactions (NSI) and analyze their impact on the determination of the NMO in NOνA and T2K. We find that NSI make the current indication in favor of NO evanescent, and therefore very fragile. More

specifically, we find that the present indication is completely erased in the presence of NSI of the flavor changing type involving the $e - \tau$ flavors [6].

Theoretical framework.—NSI may represent the low-energy manifestation of high-energy physics involving new heavy states (for a review see [7–11]) or, alternatively, they can be connected to new light mediators [12,13]. As first recognized in [14], NSI can modify the dynamics [14–16] of the neutrino flavor conversion in matter. For prospective studies of NSI at LBL experiments see [17–39]. The NSI can be described by a dimension-six operator [14]

$$\mathcal{L}_{\text{NC-NSI}} = -2\sqrt{2}G_F \varepsilon_{\alpha\beta}^{fC}(\bar{\nu}_\alpha \gamma^\mu P_L \nu_\beta)(\bar{f}\gamma_\mu P_C f), \quad (1)$$

where $\alpha, \beta = e, \mu, \tau$ refer to the neutrino flavor, $f = e, u, d$ indicate the matter fermions, superscript $C = L, R$ denotes the chirality of the ff current, and $\varepsilon_{\alpha\beta}^{fC}$ are the strengths of the NSI. The hermiticity of the interaction requires

$$\varepsilon_{\beta\alpha}^{fC} = (\varepsilon_{\alpha\beta}^{fC})^*. \quad (2)$$

For neutrino propagation in Earth matter, the relevant combinations are

$$\varepsilon_{\alpha\beta} \equiv \sum_{f=e,u,d} \varepsilon_{\alpha\beta}^f \frac{N_f}{N_e} \equiv \sum_{f=e,u,d}(\varepsilon_{\alpha\beta}^{fL} + \varepsilon_{\alpha\beta}^{fR})\frac{N_f}{N_e}, \quad (3)$$

where N_f is the number density of fermion f. For the Earth, we can assume neutral and isoscalar matter, implying $N_n \simeq N_p = N_e$, in which case $N_u \simeq N_d \simeq 3N_e$. Therefore,

$$\varepsilon_{\alpha\beta} \simeq \varepsilon_{\alpha\beta}^e + 3\varepsilon_{\alpha\beta}^u + 3\varepsilon_{\alpha\beta}^d. \quad (4)$$

The NSI affect the effective Hamiltonian for neutrino propagation in matter, which in the flavor basis becomes

$$H = U \begin{bmatrix} 0 & 0 & 0 \\ 0 & k_{21} & 0 \\ 0 & 0 & k_{31} \end{bmatrix} U^\dagger + V_{CC} \begin{bmatrix} 1+\varepsilon_{ee} & \varepsilon_{e\mu} & \varepsilon_{e\tau} \\ \varepsilon_{e\mu}^* & \varepsilon_{\mu\mu} & \varepsilon_{\mu\tau} \\ \varepsilon_{e\tau}^* & \varepsilon_{\mu\tau}^* & \varepsilon_{\tau\tau} \end{bmatrix}, \quad (5)$$

where U is the Pontecorvo-Maki-Nakagawa-Sakata matrix, which, in its standard parametrization, depends on three mixing angles (θ_{12}, θ_{13}, θ_{23}) and the CP-phase δ. The quantities $k_{21} \equiv \Delta m_{21}^2/2E$ and $k_{31} \equiv \Delta m_{31}^2/2E$ represent the solar and atmospheric wave numbers, having defined $\Delta m_{ij}^2 \equiv m_i^2 - m_j^2$, while V_{CC} is the charged-current matter potential

$$V_{CC} = \sqrt{2}G_F N_e \simeq 7.6 Y_e \times 10^{-14} \left[\frac{\rho}{\text{g/cm}^3}\right] \text{ eV}, \quad (6)$$

where $Y_e = N_e/(N_p + N_n) \simeq 0.5$ is the relative electron number density in the Earth crust. For convenience we introduce the dimensionless quantity $v = V_{CC}/k_{31}$, which gauges the sensitivity to matter effects. Its absolute value

$$|v| = \left|\frac{V_{CC}}{k_{31}}\right| \simeq 8.8 \times 10^{-2} \left[\frac{E}{\text{GeV}}\right], \quad (7)$$

will appear in the analytical expressions of the $\nu_\mu \rightarrow \nu_e$ transition probability. We here note that in T2K and NOνA the first oscillation maximum is achieved respectively for $E \simeq 0.6$ GeV ($E \simeq 1.6$ GeV). This implies that matter effects are a factor of three bigger in NOνA ($v \simeq 0.14$) than in T2K ($v \simeq 0.05$).

In the present Letter, we consider flavor nondiagonal NSI, that is $\varepsilon_{\alpha\beta}$s with $\alpha \neq \beta$. In particular, we focus on the couplings $\varepsilon_{e\mu}$ and $\varepsilon_{e\tau}$, which, as will we discuss in detail, lead to a dependency on their associated CP phase in the appearance $\nu_\mu \rightarrow \nu_e$ probability [40]. We show the results only for $\varepsilon_{e\tau}$, while we will comment about the results obtained for $\varepsilon_{e\mu}$. We recall that the current upper bounds (at 90% C.L.) on the two NSI under consideration are $|\varepsilon_{e\mu}| \lesssim 0.12$ and $|\varepsilon_{e\tau}| \lesssim 0.36$ as reported in the review [7], which refers to the global analysis [41]. These limits are basically corroborated by the more recent analysis [39]. Here an important caveat is in order. One should note that the upper bound on $|\varepsilon_{e\tau}|$ found in the global analysis performed in [39] depends on the dataset used for the experiments T2K and NOνA, which is very sensitive to such parameter. In [39] an older dataset is used compared with that adopted in the present analysis. As we will see below, the new dataset leads (in IO) to a significant preference for a nonzero value of $|\varepsilon_{e\tau}|$. As a consequence its inclusion in the global analysis would imply a sensible relaxation of the upper bound on such a parameter.

Let us consider the transition probability relevant for the LBL experiments T2K and NOνA. In the presence of NSI, the probability can be approximated as the sum of three terms [42]

$$P_{\mu e} \simeq P_0 + P_1 + P_2, \quad (8)$$

which, adopting a notation similar to [23], take the following expressions [43]

$$P_0 \simeq 4 s_{13}^2 s_{23}^2 f^2, \quad (9)$$

$$P_1 \simeq 8 s_{13} s_{12} c_{12} s_{23} c_{23} \alpha f g \cos(\Delta + \delta), \quad (10)$$

$$P_2 \simeq 8 s_{13} s_{23} v |\varepsilon| [a f^2 \cos(\delta + \phi) + b f g \cos(\Delta + \delta + \phi)], \quad (11)$$

where $\Delta \equiv \Delta m_{31}^2 L/4E$ is the atmospheric oscillating frequency, L being the baseline and E the neutrino energy, and $\alpha \equiv \Delta m_{21}^2/\Delta m_{31}^2$. For compactness, we have used the notation ($s_{ij} \equiv \sin\theta_{ij}$, $c_{ij} \equiv \cos\theta_{ij}$), and following [44], we have introduced

$$f \equiv \frac{\sin[(1-v)\Delta]}{1-v}, \qquad g \equiv \frac{\sin v\Delta}{v}. \quad (12)$$

In Eq. (11) we have assumed for the NSI coupling the general complex form

$$\varepsilon = |\varepsilon| e^{i\phi}. \quad (13)$$

The expression of P_2 is slightly different for $\varepsilon_{e\mu}$ and $\varepsilon_{e\tau}$ and, in Eq. (11), one has to make the substitutions

$$a = s_{23}^2, \qquad b = c_{23}^2 \quad \text{if } \varepsilon = |\varepsilon_{e\mu}| e^{i\phi_{e\mu}}, \quad (14)$$

$$a = s_{23} c_{23}, \qquad b = -s_{23} c_{23} \quad \text{if } \varepsilon = |\varepsilon_{e\tau}| e^{i\phi_{e\tau}}. \quad (15)$$

In the expressions given in Eqs. (9)–(11) for P_0, P_1, and P_2, the sign of Δ, α, and v are positive (negative) for NO (IO). Finally, we stress that the expressions of the transition probability provided above are valid for neutrinos and that the corresponding expressions for antineutrinos are obtained by flipping in Eqs. (9)–(11) the sign of all the CP phases and of the matter parameter v.

From the explicit expression of P_0 and P_1 one can recognize that their sum returns the standard three-flavor probability while the third term P_2 is driven by NSI. Now, we can note that the mixing angle θ_{13}, the parameter v and the coupling $|\varepsilon|$ are small and have similar size [45] ~0.2, and therefore they can be considered approximately of the same order of magnitude $\mathcal{O}(\epsilon)$, while $\alpha \equiv \Delta m_{21}^2/\Delta m_{31}^2 = \pm 0.03$ is $\mathcal{O}(\epsilon^2)$. We observe that P_0 is positive definite and independent of the CP phases, and being $\mathcal{O}(\epsilon^2)$, it provides the leading contribution to the probability. The two terms P_1 and P_2 are $\mathcal{O}(\epsilon^3)$ and are subleading. In P_1 one recognizes the standard three-flavor interference term among the atmospheric and the solar frequencies. The third term P_2 brings the dependency on the (complex) NSI coupling and it

is different from zero only in matter (i.e., if $v \neq 0$). This last term is driven by the interference of the matter potential $\varepsilon_{e\tau}V_{CC}$ with the atmospheric wave number k_{31} (see the discussion in [17]).

Data used in the analysis.—We extracted the datasets of T2K and NOνA from the latest data releases provided in [46] and [47]. The disappearance channel of T2K consists of 243 ν_μ-like (140 $\bar{\nu}_\mu$-like) events divided into 28 (19) energy bins. The appearance channel contains three event samples: 75 ν_e-like events and 15 $\bar{\nu}_e$-like events without pions, and 15 ν_e-like events with one pion in the final state. The first two samples consist of 23 bins, whereas the last one is divided into 16 bins. The dataset for the disappearance channel of NOνA is divided into four quartiles for both the neutrino and antineutrino running mode. Each quartile is divided into 19 bins. In total NOνA has observed 113 ν_μ- and 102 $\bar{\nu}_\mu$-like events. The dataset for the appearance channel is divided into three samples. Two of them are based on the particle identification variable (so-called low PID and high PID) [48,49]. The third one is the "peripheral" sample. Each of the first two samples is further divided into six bins. In total NOνA collected 58 ν_e- and 27 $\bar{\nu}_e$-like events. In our analysis we use the software GLOBES [50,51] and its additional public tool [52], which can implement NSI.

Discussion at the level of the bievents plots.—Before presenting the results of the analysis we deem it useful to discuss the interplay of the two experiments T2K and NOνA at the level of the bievents plots, in which the $x(y)$ axis reports the number of electron neutrino (antineutrino) events measured in the experiment under consideration. Such plots are particularly useful as they provide a bird eye view of the situation for each experiment and evidence possible tensions between different experiments. We recall that in the three-flavor framework the theoretical prediction, for a fixed value of the three mixing angles θ_{12}, θ_{13}, θ_{23} and of the two squared-mass splittings Δm^2_{31} and Δm^2_{21}, lies on an ellipse which has as running parameter the *CP*-phase δ in the range $[0, 2\pi]$. In the plots presented below we fix the solar parameters [53] θ_{12} and Δm^2_{21} at the best fit point of the global analysis [3], while the reactor angle θ_{13} is basically fixed at the best fit value from the reactor experiments [54]. The values of the atmospheric parameters θ_{23} and Δm^2_{31} are taken at the best fit of our own analysis.

In Fig. 1 we display the ellipses and best fit points, obtained when one combines *together* the two experiments T2K and NOνA. The continuous (dashed) curves correspond to SM (SM + NSI). Let us first comment about the standard model (SM) results. One should note that each of the two experiments constrains the fit of the other one by forcing the parameters δ, θ_{23}, and Δm^2_{31} to assume a common best fit value. In particular, in the combination the *CP*-phase δ is forced (essentially driven by T2K) to remain close to $\sim 3/2\pi$. From the left plot we see that in T2K the NO best fit (red star) is closer to the data point with respect to the IO best fit (blue star). In the right panel we see
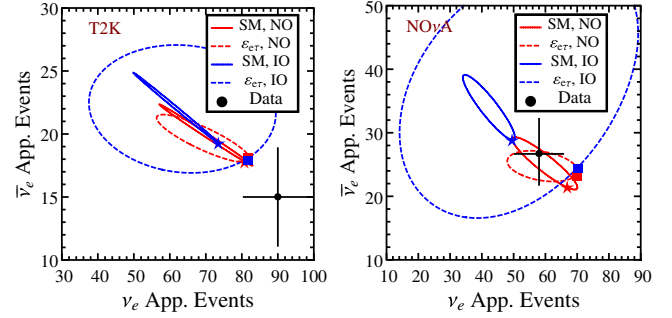

FIG. 1. Bievents plot for the T2K (left panel) and NOνA setup (right panel). The continuous (dashed) ellipse represents the parametric curve corresponding the SM (SM + NSI) case with running parameter δ in the range $[0, 2\pi]$. The ellipses and the best fit points located on them are determined by fitting the *combination* of the two experiments.

that, once the *CP*-phase δ is forced to lie close to $\sim 3/2\pi$, in NOνA there is basically no preference for any of the two hierarchies. As a result, in the overall fit, a moderate global preference for NO is obtained. We find $\chi^2_{\mathrm{SM,NO}} - \chi^2_{\mathrm{SM,IO}} \simeq -5.6$, corresponding to 2.4σ in favor of NO (see also the upper panels of Fig. 3).

In the presence of NSI the additional interference term in the transition probability provides much more freedom in the fit. In this case each pair of the NSI parameters $(|\epsilon_{e\tau}|, \phi_{e\tau})$ corresponds to a different ellipse in the bievents plot. The amplitude $|\epsilon_{e\tau}|$ influences mostly the size of the ellipse, while the phase $\phi_{e\tau}$ determines the relative length of the two axes as well as the orientation of the ellipse. The fit of the combination of T2K and NOνA selects the points (marked as squares) on those ellipses that provide the best compromise between the two experiments. In NO the best fit points in the SM + NSI have basically the same distance from the experimental data points with respect to the SM case. So we expect only a marginal improvement of the fit when including the NSI. The numerical analysis described in the next section will confirm that in NO there is indeed only a 0.7σ preference for nonzero NSI. In contrast, for IO in T2K the best fit point is much closer to the experimental point with respect to the SM case, while in NOνA the distance between best fit and data remains basically unchanged. So in IO we expect a more marked preference for NSI. The numerical analysis in the next section will confirm that in IO there is indeed a $\sim 2.5\sigma$ preference for nonzero NSI. We can also appreciate that in the SM + NSI case the distance of the best fit points (squares) from the data is basically the same in NO and IO in both experiments, so we expect a similar goodness of fit of the two mass orderings in the presence of NSI. We find $\chi^2_{\mathrm{SM+NSI,NO}} - \chi^2_{\mathrm{SM+NSI,IO}} \simeq 0.5$, corresponding to 0.7σ in favor of IO (see also the lower panels of Fig. 3). Therefore, in the presence of NSI the indication in favor of NO found in the standard case gets lost.
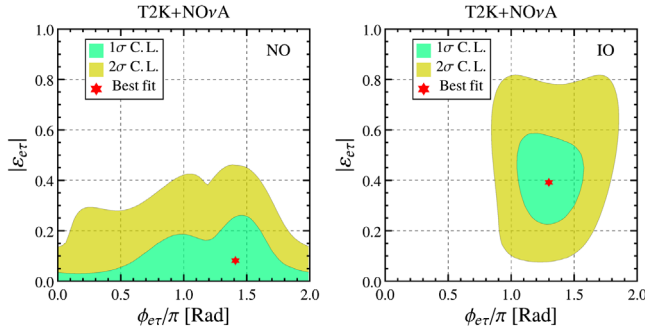
FIG. 2. Allowed regions determined by the combination of T2K and NOνA for NO (left panel) and IO (right panel). The contours are drawn at the 1σ and 2σ level for 1 d.o.f.

Numerical results.—Figure 2 reports the results of the analysis of the combination of T2K and NOνA for NO (left panel) and IO (right panel). Each panel displays the allowed region in the plane spanned by $|\epsilon_{e\tau}|$ and $\phi_{e\tau}$. The *CP*-phase δ, the mixing angles θ_{23} and θ_{13}, and the squared-mass Δm^2_{31} are marginalized away. We show the contours at the 1σ and 2σ level for 1 d.o.f. and indicate with a star the best fit point. From the left panel we can appreciate that in NO there is only a weak preference ($\simeq 0.7\sigma$) level for a nonzero value of the coupling $|\epsilon_{e\tau}|$, with best fit $|\epsilon_{e\tau}| \simeq 0.09$. In the right panel we see that the preference for nonzero NSI is stronger, reaching the 2.5σ significance with a best fit value $|\epsilon_{e\tau}| \simeq 0.39$. In NO (IO) the *CP*-phase $\phi_{e\tau}$ has best fit value 1.42π (1.30π).

In Fig. 3 we show the estimates of the two parameters δ and θ_{23}. The two upper (lower) panels report the χ^2 expanded around the minimum value obtained when the SM (SM + NSI) hypothesis is accepted as true. In each panel we display the results obtained by the combination of T2K and NOνA in NO (continuous lines) and IO (dashed lines). The undisplayed parameters are marginalized away. We observe that in the SM case there is a preference for NO at the $\sim 2.4\sigma$ level. This preference is completely washed out in the presence of NSI (lower panels), in which case there is even a mild preference for IO (at $\sim 0.7\sigma$). Therefore, we conclude that the current indication in favor of NO is fragile with respect to the perturbations induced by the NSI under study. From the left panels we can observe that the reconstruction of δ deteriorates in the presence of NSI. Notably, the values of δ close to $\pi/2$ are rejected at a much lower statistical level with respect to the SM case ($\sim 3\sigma$ instead of $\sim 5\sigma$). In addition, in the presence of NSI the *CP* conserving values $\delta = (0, \pi)$ are rejected at a lower confidence level. Concerning θ_{23} we see that in the SM case (right upper panel) there is a moderate preference for nonmaximal mixing ($\Delta\chi^2 \simeq 2.1$) and for the higher octant, the symmetric value of the best fit point in the lower octant ($\sin^2\theta_{23} \simeq 0.45$) being markedly disfavored ($\Delta\chi^2 \simeq 4.5$). In the presence of NSI both the preference for a nonmaximal mixing and that for the higher octant found in the SM
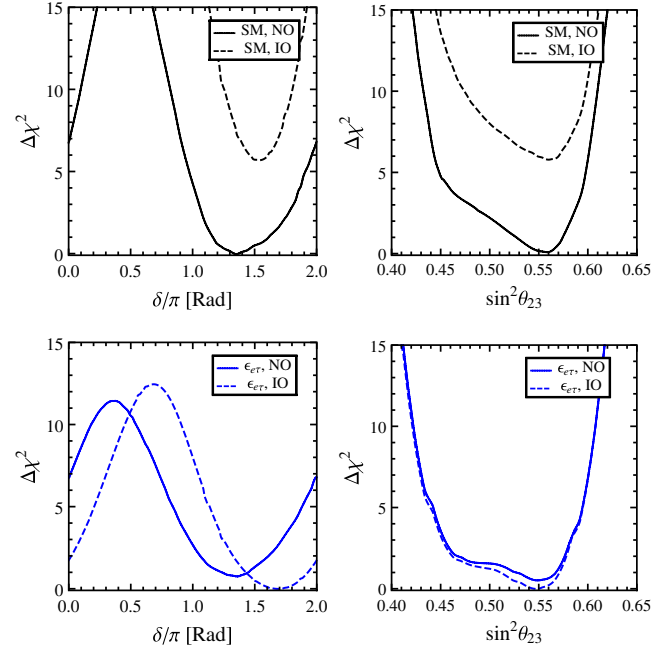

FIG. 3. Estimates of δ and θ_{23} for SM (upper panels) and SM + NSI (lower panels) determined by the combination of T2K and NOνA. The continuous (dashed) curves refer to NO (IO).

sensibly decrease. In this case maximal mixing is disfavored only at $\Delta\chi^2 \simeq 1.3$ and the lower octant at $\Delta\chi^2 \simeq 2.9$.

It is worthwhile to make some comments on the results of the analysis obtained considering the interaction in the $e - \mu$ sector. Differently from the $e - \tau$ sector we find a significant preference for nonzero values of $|\epsilon_{e\mu}|$ both in NO and IO. We obtain best fit value $|\epsilon_{e\mu}| = 0.15$ ($|\epsilon_{e\mu}| = 0.10$) for NO (IO) with statistical significance of 1.6σ (1.5σ). The corresponding best fit value of the *CP*-phase $\phi_{e\mu}$ is 1.78π (1.82π) for NO (IO). Since there is approximately the same improvement of the fit in NO and IO, the indication in favor of NO remains almost unaltered with respect to the SM case. In fact, we find that NO is preferred over IO at the 2.5σ level similar to the SM case. Therefore, the fragility of the indication in favor of the NO appears only when considering the nonstandard interactions in the $e - \tau$ sector.

In this Letter we have focused on the real data provided by NOνA and T2K. Needless to say, it is interesting to consider the impact of the degeneracy problem we have found in real data on the future LBL experiments, which are expected to have a higher sensitivity to the NMO. In the Supplemental Material [55] (which includes Refs. [50–52,56–60]), we show explicitly what may be expected from DUNE. Here, we limit ourselves to summarize the basic result, by stating that the degeneracy issue under consideration can be resolved by DUNE only if δ will be confirmed to lie sufficiently close to its current best fit value $\delta \sim 1.5\pi$. Also we have checked that ESSνSB, T2HK and T2HKK will have less chances to resolve the issue with respect to DUNE.

Conclusions.—In this Letter we have investigated the impact of NSI on the interpretation of T2K and NOνA data. Our main result is that the indication in favor of NO valid in the standard three-flavor scheme does not hold anymore if one assumes the existence of neutral-current nonstandard interactions of the flavor changing type involving the $e - \tau$ ($\varepsilon_{e\tau}$) flavors. We have also investigated the potential role of the future LBL experiment DUNE in resolving the degeneracy issue that plagues the present data. An unambiguous determination of the NMO in the presence of NSI will be possible only if the *CP*-phase δ will be confirmed to lie not too far from the present best fit value around $\delta \sim 1.5\pi$. We conclude this letter by underlining that, apart from the LBL accelerator data, it would be very interesting to complement our study considering the existing and future atmospheric neutrino data, which may help to resolve the NMO ambiguity. Finally, our work clearly evidences the importance of investigating the NMO exploiting different types of experiments, such as JUNO, which are less sensitive to (standard and non-standard) matter effects.

[*]capozzi@mpp.mpg.de
[†]sabya.s.chatterjee@durham.ac.uk
[‡]palazzo@ba.infn.it

[1] In our present analysis, which makes use of the latest T2K T2K_talk and NOνA [47] data releases, we find that the indication in favor of NO is now at the $\sim 2.4\sigma$ level.
[2] K. Abe *et al.* (Super-Kamiokande Collaboration), Phys. Rev. D **97**, 072001 (2018).
[3] F. Capozzi, E. Lisi, A. Marrone, and A. Palazzo, Prog. Part. Nucl. Phys. **102**, 48 (2018).
[4] P. F. de Salas, D. V. Forero, C. A. Ternes, M. Tortola, and J. W. F. Valle, Phys. Lett. B **782**, 633 (2018).
[5] I. Esteban, M. C. Gonzalez-Garcia, A. Hernandez-Cabezudo, M. Maltoni, and T. Schwetz, J. High Energy Phys. 01 (2019) 106.
[6] We stress that the confusion problem we are pointing out is not related to the so-called generalized mass ordering degeneracy recently identified in Ref. [61] (see also Ref. [62]), which arises for the very large values of the NSI couplings (specifically $\epsilon_{ee} \sim -2$) needed to accommodate the dark LMA solution [63] to the solar neutrino problem.
[7] Y. Farzan and M. Tortola, Front. Phys. **6**, 10 (2018).
[8] C. Biggio, M. Blennow, and E. Fernandez-Martinez, J. High Energy Phys. 08 (2009) 090.
[9] T. Ohlsson, Rep. Prog. Phys. **76**, 044201 (2013).
[10] O. G. Miranda and H. Nunokawa, New J. Phys. **17**, 095002 (2015).
[11] P. S. B. Dev *et al.*, Sci. Post. Phys. Proc. **2**, 001 (2019).
[12] Y. Farzan, Phys. Lett. B **748**, 311 (2015).
[13] Y. Farzan and I. M. Shoemaker, J. High Energy Phys. 07 (2016) 033.
[14] L. Wolfenstein, Phys. Rev. D **17**, 2369 (1978).
[15] S. Mikheev and A. Y. Smirnov, Sov. J. Nucl. Phys. **42**, 913 (1985).
[16] S. Mikheev and A. Y. Smirnov, Nuovo Cimento C **9**, 17 (1986).
[17] A. Friedland and I. M. Shoemaker, arXiv:1207.6642.
[18] J. A. B. Coelho, T. Kafka, W. A. Mann, J. Schneps, and O. Altinok, Phys. Rev. D **86**, 113015 (2012).
[19] Z. Rahman, A. Dasgupta, and R. Adhikari, J. Phys. G **42**, 065001 (2015).
[20] P. Coloma, J. High Energy Phys. 03 (2016) 016.
[21] A. de Gouvêa and K. J. Kelly, Nucl. Phys. **B908**, 318 (2016).
[22] S. K. Agarwalla, S. S. Chatterjee, and A. Palazzo, Phys. Lett. B **762**, 64 (2016).
[23] J. Liao, D. Marfatia, and K. Whisnant, Phys. Rev. D **93**, 093016 (2016).
[24] D. V. Forero and P. Huber, Phys. Rev. Lett. **117**, 031801 (2016).
[25] K. Huitu, T. J. Kärkkäinen, J. Maalampi, and S. Vihonen, Phys. Rev. D **93**, 053016 (2016).
[26] P. Bakhti and Y. Farzan, J. High Energy Phys. 07 (2016) 109.
[27] M. Masud and P. Mehta, Phys. Rev. D **94**, 013014 (2016).
[28] C. Soumya and R. Mohanta, Phys. Rev. D **94**, 053008 (2016).
[29] M. Masud and P. Mehta, Phys. Rev. D **94**, 053007 (2016).
[30] A. de Gouvêa and K. J. Kelly, arXiv:1605.09376.
[31] S. Fukasawa, M. Ghosh, and O. Yasuda, Phys. Rev. D **95**, 055005 (2017).
[32] J. Liao, D. Marfatia, and K. Whisnant, J. High Energy Phys. 01 (2017) 071.
[33] J. Liao, D. Marfatia, and K. Whisnant, Phys. Lett. B **767**, 350 (2017).
[34] M. Blennow, S. Choubey, T. Ohlsson, D. Pramanik, and S. K. Raut, J. High Energy Phys. 08 (2016) 090.
[35] K. N. Deepthi, S. Goswami, and N. Nath, Nucl. Phys. **B936**, 91 (2018).
[36] L. J. Flores, E. A. Garces, and O. G. Miranda, Phys. Rev. D **98**, 035030 (2018).
[37] J. M. Hyde, Nucl. Phys. **B949**, 114804 (2019).
[38] M. Masud, S. Roy, and P. Mehta, Phys. Rev. D **99**, 115032 (2019).

[39] I. Esteban, M. C. Gonzalez-Garcia, and M. Maltoni, J. High Energy Phys. 06 (2019) 055.

[40] The $\nu_\mu \to \nu_\mu$ disappearance channel is sensitive to the $\mu - \tau$ coupling but this can be safely ignored because of the very strong upper bound coming from the atmospheric neutrinos $|\epsilon_{\mu\tau}| < 8.0 \times 10^{-3}$ [64] (see also Ref. [65]).

[41] M. C. Gonzalez-Garcia and M. Maltoni, J. High Energy Phys. 09 (2013) 152.

[42] T. Kikuchi, H. Minakata, and S. Uchinami, J. High Energy Phys. 03 (2009) 114.

[43] Interestingly, a similar decomposition of the conversion probability holds in the presence of a light sterile neutrino [66]. In that case, however, the nature of the new interference term P_2 is kinematical, and it is operative also in vacuum. In fact, the new term is due to the interference of the atmospheric oscillations with those induced by the new large squared-mass splitting related to the sterile state.

[44] V. Barger, D. Marfatia, and K. Whisnant, Phys. Rev. D **65**, 073023 (2002).

[45] Here we are anticipating that the numerical analysis presented below points toward best fit values in the range $|\epsilon| \sim 0.1$–0.4.

[46] G. Żarnecki, in Proceedings at Les Rencontres de Physique de la Valle d'Aoste, 2019, La Thuile, Italy, 2019.

[47] M. A. Acero et al. (NOvA Collaboration), Phys. Rev. Lett. **123**, 151803 (2019).

[48] A. Aurisano, A. Radovic, D. Rocco, A. Himmel, M. D. Messier, E. Niner, G. Pawloski, F. Psihas, A. Sousa, and P. Vahle, J. Instrum. **11**, P09001 (2016).

[49] F. Psihas, E. Niner, M. Groh, R. Murphy, A. Aurisano, A. Himmel, K. Lang, M. D. Messier, A. Radovic, and A. Sousa, Phys. Rev. D **100**, 073005 (2019).

[50] P. Huber, M. Lindner, and W. Winter, Comput. Phys. Commun. **167**, 195 (2005).

[51] P. Huber, J. Kopp, M. Lindner, M. Rolinec, and W. Winter, Comput. Phys. Commun. **177**, 432 (2007).

[52] J. Kopp, https://www.mpi-hd.mpg.de/personalhomes/globes/tools/snu-1.0.pdf (2010).

[53] We recall that θ_{12} and Δm_{21}^2 are determined by the combination of solar and Kamland data.

[54] Technically we treat θ_{13} as a free parameter taking into account the strong prior coming from the reactor experiments (dominated by Daya Bay).

[55] See the Supplemental Material at http://link.aps.org/supplemental/10.1103/PhysRevLett.124.111801 for the capability of future LBL experiments to resolve the NMO confusion issue generated by the presence of NSI.

[56] R. Acciarri et al. (DUNE Collaboration), arXiv:1512.06148.

[57] K. Abe et al. (Hyper-Kamiokande Proto-Collaboration), Prog. Theor. Exp. Phys. **2015**, 053C02 (2015).

[58] K. Abe et al. (Hyper-Kamiokande Collaboration), Prog. Theor. Exp. Phys. **2018**, 063C01 (2018).

[59] E. Baussan et al. (ESSnuSB Collaboration), Nucl. Phys. **B885**, 127 (2014).

[60] T. Alion et al. (DUNE Collaboration), arXiv:1606.09550.

[61] P. Coloma and T. Schwetz, Phys. Rev. D **95**, 079903 (2017).

[62] P. Bakhti and Y. Farzan, J. High Energy Phys. 07 (2014) 064.

[63] O. G. Miranda, M. A. Tortola, and J. W. F. Valle, J. High Energy Phys. 10 (2006) 008.

[64] IceCube, M. G. Aartsen et al., Phys. Rev. D **97**, 072009 (2018).

[65] Super-Kamiokande, G. Mitsuka et al., Phys. Rev. D **84**, 113008 (2011).

[66] N. Klop and A. Palazzo, Phys. Rev. D **91**, 073017 (2015).